31st Annual International Conference of the IEEE EMBS
Minneapolis, Minnesota, USA, September 2-6, 2009

Monitoring and Guidance of Minimally-Invasive Thermal Therapy Using Diagnostic Ultrasound

Emad S. Ebbini and John C. Bischof

Abstract— **We present specialized ultrasound imaging modes for monitoring and guidance of noninvasive and minimally-invasive thermal therapy. One mode is based on two-dimensional imaging of temperature change using diagnostic ultrasound. We have validated this method both *in vivo* and *in vitro* in monitoring the heating patterns produced by noninvasive HIFU source and minimally-invasive RF ablation device, respectively. In addition, a nonlinear method for imaging the quadratic echo components from HIFU-induced lesions has also been developed and tested *in vivo*. Illustrative results from both modes of imaging are presented. These results demonstrate the unique advantages of ultrasound as an image-guidance modality. Specifically, the high spatial and temporal resolutions that allow for imaging highly-localized short-duration therapeutic and sub-therapeutic HIFU beams. With the advent of high-performance computing hardware, these imaging modes are now implementable in real-time. This will lead to active real-time monitoring and control of a range of thermal therapies in the very near future.**

I. INTRODUCTION

Ultrasound imaging continues to be an attractive modality for guidance and monitoring of noninvasive and minimally invasive thermal therapies, e.g. RF ablation and high intensity focused ultrasound (HIFU). The main advantages of ultrasound as an image guidance modality are its real-time nature, its cost effectiveness and ease of integration with other instrumentation. In its conventional B-mode, it offers high spatial and temporal resolution and reasonable contrast resolution in target tissues like the liver (RF ablation) and prostate (HIFU). Recently, advances in real-time signal processing hardware have enabled the implementation of several specialized imaging modes that will undoubtedly increase the attractiveness of ultrasound as an image guidance modality, especially in conjunction with HIFU. These methods include:

1) Imaging of temperature change: This may be the most significant feature in monitoring and guidance of thermal therapy. In addition to providing feedback on the tissues thermal response to the therapeutic beam, it may be used in guiding the therapy at sub-therapeutic exposure levels.
2) Imaging nonlinear echo components due to cavitation and/or tissue boiling. These are very useful feedback parameters that may help characterize high or excessive exposure levels.
3) Elastography and acoustic radiation force methods: These methods offer the promise of high contrast imaging of material properties relevant to tissue changes associated with induced thermal lesions. Specifically, it is well accepted that the stiffness of the tissue increases upon protein coagulation.

We have developed and validated all three forms of imaging *in vitro* freshly excised tissue samples undergoing HIFU or RF ablation treatment . Preliminary *in vivo* results have also been obtained on nonlinear imaging [1]. In this paper, we report *in vivo* results of temperature imaging of tissue undergoing sub-therapeutic HIFU exposure (for guidance purposes).

Several methods have been proposed for temperature imaging using pulse-echo ultrasound, but echo shift estimation (using speckle tracking [2], [3], [4]) and spectral shift estimation (using high resolution spectral estimation [5]) are most commonly used methods. The principle of measurement was validated experimentally by several groups in tissue and tissue-mimicking samples [6], [7], [8]. Both spectral and echo shift models for estimation of temperature change employed a linear model with a proportionality "constant" related to the temperature coefficient of the speed of sound, $\beta = (\partial c/\partial T)/c$, and the coefficient of thermal expansion, α [9]. These methods, however, currently suffer from some limitations that have hindered their adoption in the clinic. These limitations stem from native tissue deformations (e.g. due to breathing and cardiac cycle) leading to echo and spectral shifts easily masking the (typically very small) temperature-induced shifts. Heterogeneities in the target tissue as well as the scattering models could result in misinterpretation of the temperature-induced shifts. Tissue strains due to fast switching of the heating source (as in pulsed HIFU or on/off control of RF ablation) also produce artifacts due to undersampling of the tissue displacement fields at typical frame rates of 2D ultrasound imaging.

In this paper, we present preliminary data to demonstrate that the above limitations do not represent insurmountable challenges to robust temperature estimation using pulse-echo ultrasound. Conquering these limitations, however, requires innovative solutions employing new approaches to data acquisition and reconstructive temperature estimation. These innovations are made possible by the availability of programmable scanners and high-performance computing hardware enabling correlation-based real-time speckle tracking matching the spatial and temporal resolution of the ultrasound imaging system. We propose a new "system" for robust, real-time, noninvasive 2D temperature estimation.

This work is funded in part by Grants EB 004456 and EB 006893 from the National Institutes of Health

E.S. Ebbini is with the Department of Electrical and Computer Engineering, University of Minnesota Twin Cities emad@umn.edu

J.C. Bischof is with the Department of mechanical Engineering, University of Minnesota Twin Cities bischof@umn.edu

978-1-4244-3296-7/09/$25.00 ©2009 IEEE

II. Results

A. Temperature Estimation

In most tissue media around body temperature, c increases with temperature in the range (see [10]). In fatty tissues, c decreases with increasing temperature[11].

In [5], we have described a temperature measurement equation of the form:

$$\Delta f_k(T) \approx \frac{k}{2}\left[\frac{\partial c(T)}{\partial T}\frac{1}{d(T)}|_{T=T_0} - \frac{\partial d(T)}{\partial T}|_{T=T_0}\frac{c(T)}{d^2(T)}\right]\Delta T, \qquad (1)$$

which relates the change in tissue temperature to changes in harmonic frequencies related to the mean scatterer spacing [12]. The above equation was derived from an assumed semi-regular scattering model, which related the mean scatterer spacing, $d(T)$, to harmonically related peaks in the echo spectrum at $f_k = \frac{kc(T)}{2d(T)}$.

Strictly speaking, the baseline temperature, T_0, is a function of space and time. However, in practice, the proportionality constant in (1) is constant for a range of ΔT up to 15 °C from normal body temperature. Therefore, it is reasonable to assume T_0 constant throughout the temperature range of interest.

Taking $c(T)/d(T)$ as a common factor outside the brackets, (1) can be written in the form

$$\Delta T(z) = \left[\frac{1}{\beta - \alpha}\right]\frac{\Delta f_k}{f_k}, \qquad (2)$$

where $\alpha = (\partial d(T)/\partial T)/d(T)$ is the linear coefficient of thermal expansion and $\beta = (\partial c(T)/\partial T)/c(T)$ is the thermal coefficient of the speed of sound.

Note that for values of ΔT higher the 20 °C, the whole approach based on echo ultrasound is likely to fail. Under such conditions, one may want to account for T_0 as a function of time and space.

In [2], we have described a temperature estimation algorithm based on speckle tracking relating changes in echo location to changes of tissue temperature. This approach was extended and fully described in [4]. It has been shown in [4] that

$$\Delta T(z) = \frac{c(T_0)}{2}\left[\frac{1}{\beta - \alpha}\right]\frac{\partial}{\partial z}(\delta t(z)). \qquad (3)$$

Not surprisingly, the proportionality is determined by the same parameters that determined the frequency shift in (1). For a homogeneous medium these parameters can be determined experimentally. Therefore, (3) suggests that temperature-change estimates can be obtained by first tracking the cumulative echo time-shift at each location, and then differentiating along the axial direction z and filtering along both axial and lateral x directions. This method was explained and discussed in detail in [4]. Alternatively, (1) suggests that temperature change estimates can be obtained from relative frequency shifts at selected frequencies in the echo spectrum. A comparison between the spectral domain and the time domain methods described in this section can be found in [9].

1) 2D Spatial Filtering: In [4], we have proposed a 2D spatial filter to obtain well-behaved temperature estimation results relatively free of thermoacoustic lens effects. This approach was shown to be effective in reducing the thermoacoustic lens effects. recently, we have introduced a time-varying 2D Gaussian-like filter for post processing of the (noisy and artifact-ridden) temperature estimates. This filter is obtained from the Green's function of the transient bioheat transfer equation (tBHTE). The cutoff frequencies of the filter are reduced as a function of time after the heating source is switched on. This accounts for the smoothing of the heating profile due to heat conduction, which results from the parabolic nature of the tBHTE.

$$h(\vec{r},t) = \frac{1}{(4\kappa(t-t_0))^{n/2}}\; e^{-\frac{|\vec{r}|^2}{2\kappa(t-t_0)}}, \qquad (4)$$

where $\kappa = K/\rho C$ is related to the thermal diffusivity (K conductivity, ρ density, and C heat capacity), t_0 is the switch-on time and $n = 1,2,3$ is the order of the filter determined by the number of spatial coordinates observed by the ultrasound imaging system. For illustration, we have used this filter with the M-mode spatio-temporal data ($n = 1$) in Section II-B and 2D data ($n = 2$) in Section **??** below.

2) Iterative Reconstruction: Various factors contributing to artifacts in displacement estimation are encountered in practice. In addition to the thermoacoustic lens effect, motion and deformation of the tissue undergoing heating, spatial inhomogeneity and anisotropy of the temperature dependence are some of the more obvious ones. These artifacts may lead to unrealistic temperature estimates at some locations, e.g. cooling in a heated region. These effects can be mitigated by an iterative reconstruction algorithm that enforces the non-negativity constraint $\Delta T \geq 0$ in the spatial coordinates and applies the (tBHTE-based) time-varying Gaussian filter described above to the temperature estimate obtained using (1) or (3). This procedure is repeated until the temperature field converges as a form of projection onto convex sets (POCS) [13] with basic iteration:

$$T_{k+1}(x,z,t) = \mathscr{G}(t)\mathscr{P}T_k(x,z,t), \qquad (5)$$

where $T_k(x,z,t)$ is the kth reconstruction of the 2D temperature at time t. The projection operator, $\mathscr{G}(t)$, is the time-varying, bandlimiting Gaussian-like filter defined in (4). The projection operator, $\mathscr{P}$, is the non-negativity constraint operator $T = max\{T,0\}$. The main advantage of this approach is the removal of artifacts from the estimated temperature profile without excessive smoothing due to lowpass filtering as illustrated below.

B. Experimental Results: In Vivo Tumor Model in Nude Mouse

Lesion formation experiments in the hind limb of tumor bearing nude mice were performed using the 4-MHz HIFU transducer (Focus Surgery, Inc., Indianapolis, IN) and were monitored using the Technos MPX ultrasound scanner (Esaote S.p.A, Genoa, Italy). The HIFU transducer was positioned so that its focal point intersects the imaging plane

of the imaging probe as shown in Figure 1. A linear array probe (LA522E, 2-cycle transmit pulse centered at 5.5 MHz) was used to collect RF data for temperature estimation at 89 fps. Two seconds of frame data were collected before, during, and after short (0.2 seconds), sub-therapeutic HIFU exposures for the purpose of localization of the heating spot as well as the transient response to the HIFU beam. This form of feedback could provide the key to successful calibration of the HIFU source *in situ* before delivering the therapeutic HIFU pulse. Figure 2(a) illustrates the procedure using the direct temperature measurements obtained using a luxtron fiberoptic probe positioned in the vicinity of the HIFU focus. The top panel shows a recording of the temperature history of the experiment. The lower panels show the temperature rise curves due to a sub-therapeutic HIFU shot (left: 0.2 seconds, 5.4 Watt), an ablative HIFU shot (center: 5 seconds, 48 Watt), and another sub-therapeutic shot (right: 0.2 seconds, 5.4 Watt). This procedure represents one scenario for the use of temperature feedback to characterize the tissue response before and after ablation. For example, the tissue response to the sub-therapeutic HIFU shot after lesion formation clearly demonstrates increased absorption ($\approx$ 3-fold increase in ΔT in response to the same incident power) and decreased perfusion (as evidenced by the decreased rate of decay compared to the pre-lesion sub-therapeutic HIFU shot).

A pointer was used to locate the HIFU focus on the Technos MPX image. For the experiments described herein, the HIFU transducer and the LA522E probe were fixed on the same holder (once the HIFU focus was positioned at a known point on the Technos MPX image). The transducer assembly was then positioned so that the HIFU focus is at the center of the tumor. Figure 1 shows a B-mode image obtained by the Technos MPX using the LA522E probe. The image size is 2 cm by 4.1 cm and shows an approximately circular cross section of the tumor near the top with the thigh directly below and part of the pelvis to the left.

Figure 2 (b) illustrates the temperature-induced echo and spectral shift phenomena observed in the pulse-echo RF data. The top panel show two 31-sample segments of A-line data acquired through the heated spot generated by the therapeutic transducer in Figure 1. A small shift between the A-lines can be observed from the raw RF data. Using complex cross correlation (middle panel), we are able to estimate the time shift with sub-sample accuracy without the need for interpolation. In this case, the echo shift is only 0.2 sample time ($F_s = 33$ MHz) or nearly 6 nanoseconds or, equivalently, a spatial shift of 4.55 μsec (assuming a speed of sound of 1500 m/sec). The bottom panel shows high resolution spectral estimation from the 31-sample segments to demonstrate the temperature-induced spectral shifts. One can observe two spectral peaks at approximately 4.6 and 5.6 MHz with spectral shifts of approximately 25 and 40 kHz, respectively.

Figure 3 (a) shows the raw spatio-temporal map of the frequency shifts obtained before, during, and after the sub-therapeutic HIFU shot delivered before lesion formation. The frequency shift profile was scaled to give estimated

Fig. 1. Left: Configuration of the integrated imaging/HIFU system showing the intersection of the imaging plane with the HIFU focus. Right: A screen capture showing a B-mode image of the tumor in the hind limb of a nude mouse.

temperature change based on typical values of $\alpha = 1 \times 10^{-4}$ and $\beta = 6.7e-4$. The results show a maximum temperature change at the HIFU focus of nearly 5°C. One can also observe several artifacts due to the breathing cycle leading to apparent temperature swings of ± 1.2°C. Figure 3 (b) shows a spatio-temporal map of the cross-correlation of the RF data used in computing the spectral shift map. One can see a reduction in the cross correlation coefficient at the onset of the HIFU shot (0.3 seconds and 7.5 mm axial distance). One can also observe the reduction in cross correlation due to the presence of an artery (9 mm axial distance).

Figure 4 demonstrate the use of the spatio-temporal tBHTE-based filter ($n = 1$), together with the POCS algorithm. The breathing artifacts were reduced to $0 - 0.5$°C after two iterations. A better appreciation of the workings of the POCS algorithm may be attained with the help of the lower left panel which shows the raw and filtered temperature profiles at the HIFU focus (7.5 mm axial depth). One can see the large temperature swing in the raw estimate, which is likely due to the loss of correlation at the onset of the HIFU pulse. This can be attributed to significant tissue displacement/deformation due the radiation force effects of the HIFU beam. This artifact is largely eliminated by the POCS algorithm, without overly smoothing the data.

III. Conclusions

Real-time ultrasound provides a unique method for monitoring and guidance of thermal therapy, thanks to its demonstrated ability to image 2D temperature changes in the treated region. This can be achieved with spatial and temporal resolutions unmatched by other guidance methods, e.g.

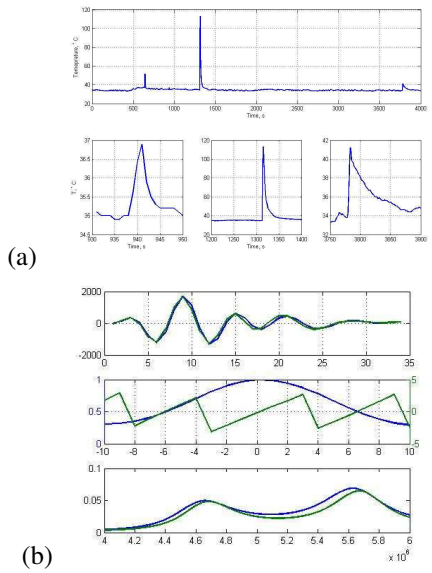

Fig. 2. Illustration of the experimental procedure using direct temperature measurements near the HIFU focus (a) and the nature of temperature-induced echo and spectral shifts in the pulse-echo RF data from the heated region (b).

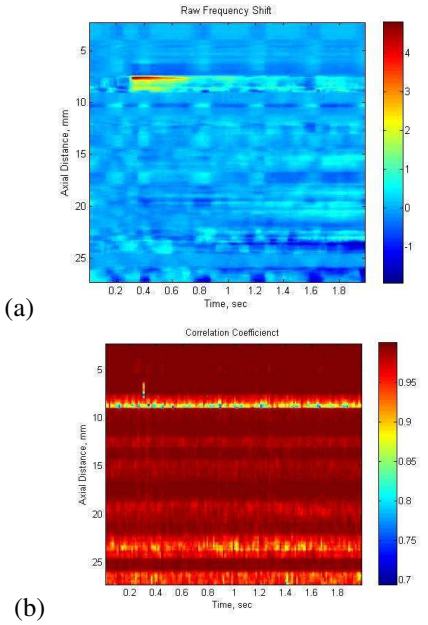

Fig. 3. (a) Spatio-temporal temperature map obtained from scaled frequency shifts obtained while monitoring a sub-therapeutic HIFU shot. (b) A spatio-temporal map of the cross correlation of the data used to obtain the frequency shift map.

MRI. Despite some limitations which are currently subject to intense research, 2D temperature change imaging with ultrasound offers the promise of guiding thermal therapy devices and local tissue property measurements which may be correlated with irreversible damage to the treated tissue. With this capability, not only will ultrasound provide monitoring and guidance modality, it will also provide a method for assessment of tissue damage to thermal ablation. Thus a complete image guidance modality of thermal therapy is feasible.

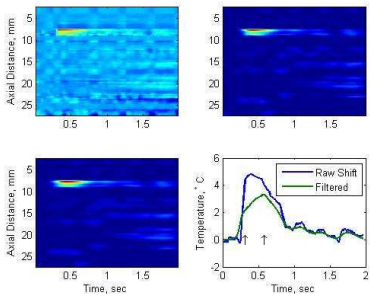

Fig. 4. Estimated spatio-temporal temperature profiles using POCS: Top Left: raw. Top Right: after the first iteration. Lower left: after two iterations. Lower Right: line plots of raw and filtered temperature profiles at 7.5 mm axial distance (HIFU focus).

IV. ACKNOWLEDGMENTS

The authors wish to thank Dr. Rachana Visaria, Dr. Robert Griffin, Dr. Hui Yao, and Mr. Ajay Shrestha for help with the animal setup used for collecting the ultrasound RF data.

REFERENCES

[1] E. S. Ebbini, J.C. Bischof, R.K. Visaria, and A. Shrestha, "Quadratic B-Mode and pulse inversion imaging of thermally-induced lesions in vivo," in *4th IEEE International Symposium on Biomedical Imaging(ISBI 2007)*, 2007, pp. 1120 – 1123.

[2] R. Seip, P. VanBaren, C. Simon, and E. Ebbini, "Non-invasive spatio-temporal temperature change estimation using diagnostic ultrasound," in *Proc. IEEE Ultrason. Symp.*, 1995, pp. 1613–1616.

[3] R. Maass-Moreno and C.A. Damianou, "Noninvasive temperature estimation in tissue via ultrasound echo shifts. part i. theoretical model," *The Journal of the Acoustical Society of America*, vol. 100, no. 4, pp. 2514–2521, 1996.

[4] C. Simon, P. VanBaren, and E.S. Ebbini, "Two-dimensional temperature estimation using diagnostic ultrasound," *IEEE Trans. UFFC*, vol. 45, pp. 989–1000, July 1998.

[5] R. Seip and E. Ebbini, "Non-invasive estimation of tissue temperature response to heating fields using diagnostic ultrasound," *IEEE Trans. Biomed. Eng.*, vol. 42, no. 8, pp. 828–839, 1995.

[6] Naomi R Miller, Jeffrey C Bamber, and Paul M Meany, "Fundamental limitations of noninvasive temperature imaging by means of ultrasound echo strain estimation," *Ultrasound in Medicine and Biology*, vol. 28, pp. 1319–1333, Oct. 2002.

[7] M. Pernot, M. Tanter, J. Bercoff, K. Waters, and M. Fink, "Temperature estimation using ultrasonic spatial compounding," *IEEE Trans. Ultrason., Ferroelect., Freq. Contr.*, vol. 51, no. 5, pp. 606 – 615, 2004.

[8] Rmi Souchon, Guillaume Bouchoux, Eva Maciejko, Cyril Lafon, Dominique Cathignol, Michel Bertrand, and Jean-Yves Chapelon, "Monitoring the formation of thermal lesions with heat-induced echo-strain imaging: A feasibility study," *Ultrasound in Medicine and Biology*, vol. 31, pp. 251–259, Feb. 2005.

[9] A. Nasiri Amini, E.S. Ebbini, and T. Georgiou, "Noninvasive Estimation of Tissue Temperature via High-Resolution Spectral Analysis Techniques," *IEEE Trans. Biomedical Engineering*, vol. 52, no. 2, pp. 221 – 228, 2005.

[10] L.E. Kinsler and A. R. Frey, *Fundamentals of Acoustics*, Wiley, New York, NY, 3rd edition, 1982.

[11] J. F. Greenleaf, P. J. Thomas, S. A. Johnson, and R. C. Bahn, "Ultrasonic Tissue Characterization II," 1979, pp. 227–233.

[12] R. Seip C. Simon, J. Shen and E. Ebbini, "A robust and computationally efficient algorithm for mean scatterer spacing estimation," *IEEE Trans. Ultrason., Ferroelect., Freq. Contr.*, vol. 44, no. 4, pp. 882–894, 1997.

[13] Ed. H. Stark, *Image Recovery: From Theory to Application*, Academic Press, New York, NY, 2nd edition, 1987.